Supplementary Information

A cross-laboratory experimental study of non-noble-metal electrocatalysts for the oxygen reduction reaction

(a) Frédéric Jaouen[*], Juan Herranz, Michel Lefèvre, Jean-Pol Dodelet; (b) Ulrike I. Kramm, Iris Herrmann, Peter Bogdanoff ; (c) Jun Maruyama[(1)], Toru Nagaoka[(2)]; (d) Arnd Garsuch, Jeff R. Dahn; (e) Tim Olson, Svitlana Pylypenko, Plamen Atanassov; (f) Eugene A. Ustinov

(a) Institut National de la Recherche Scientifique, Énergie, Matériaux & Télécommunications
 (b) Helmholtz-Zentrum Berlin GmbH
(c) Environmental Technology Research Division [(1)] and Processing Technology Research Division [(2)], Osaka Municipal Technical Research Institute
(d) Department of Physics and Atmospheric Science, Dalhousie University
(e) Chemical & Nuclear Engineering Department, University of New Mexico
 (f) Ioffe Physical Technical Institute,

A. State-of-art volumetric activity for Pt/C

The value of 1300 A cm^{-3} under conditions of 80°C and 1 bar dry O$_2$ originates from the kinetic current density I$_K$ of 1450 mA cm^{-2} at 0.8 V iR-free cell voltage (kinetic current, Fig.4, grey circles in [1] obtained with a Pt loading at the cathode of 0.4 mg cm^{-2}. The Pt catalyst is 47 wt% Pt dispersed on carbon. An effective density of 0.4 g carbon per cm^3 of electrode was assumed (usual value, coming from measurement of electrode thickness [1]. From these data, the reference Pt volumetric activity, I$_V$*, can be calculated from the following equation

$$I_V{}^* = -I_K{}^* \cdot \rho_{eff}/m_C \hspace{3cm} Eq.S1$$

Where I$_K$* (<0 for a reduction reaction) is in A cm^{-2}, ρ_{eff} is in gram of carbon black per cm^3 of porous electrode, and m$_C$ is the carbon black loading in g cm^{-2}. For 47 % Pt/C, the carbon black loading is the Pt loading x 53/47. I$_V$* is in A cm^{-3} electrode.

B. Catalyst synthesis

Approach (i) uses a metal-N$_4$ chelate as the exclusive or main precursor for metal, nitrogen and carbon. The pyrolysis is made in inert gas. In two instances (UK63, UK65), iron oxalate is added to obtain high surface areas. Catalysts made according to approach (i) are UK63, UK65, CHb200900 and CoTMPP700.

UK63 [2] (Helmholtz-Zentrum Berlin (HZB)): One gram (1.2 mmol) of FeClTMPP, 5 g of Fe oxalate dihydrate (27.8 mmol) and 0.3 g of sulphur (9.4 mmol) are mixed together in the sequence S, Fe oxalate, FeClTMPP. Before mixing, the iron oxalate had been previously ballmilled to smaller particles. The precursor is filled into a quartz boat and

introduced into a quartz glass tube and heated under constant flow of N_2 in a split-hinge furnace. The heat treatment under N_2 consists of a step at 450 °C for 15 min and a second step at 800 °C for 45 min. The heating rate is 450˚C/h. After cooling under inert gas, the catalyst is then etched in 1M HCl for 12h followed by water filtration until pH 5 is reached, and then dried. The product obtained is subject to a 2nd heat treatment: the powder is heated to 800 °C in N_2/H_2 (90/10) and stays at 800 °C for 30 min. After cooling, the sample is etched in 1M HCl. After filtration, washing and drying, the remaining powder is subject to a 3rd heat treatment: the powder is heated to 800 °C in N_2 and at 800 °C the gas is switched to CO_2 for 30 min. The cooling process is under N_2.

UK65[2] (HZB): Same as UK63 but 1.2 mmol (0.975g) CoTMPP is used instead of FeClTMPP.

CHb200900 [3] (Osaka Municipal Technical Research Institute, OMTRI): Hemoglobin from bovine blood is ground. A pyro-polymer is formed by the heat treatment of hemoglobin under flowing Ar below 600˚C for 10 h and then finely ground. The pyro-polymer is subsequently heated at 5˚C min^{-1} under a flow of 10 % CO_2 and 90 % Ar up to 900˚C and held there for 2 h. The sample is ground and acid-washed in boiling 0.5 M H_2SO_4 for 1h, followed by filtering, washing with high-purity water, and drying under vacuum at room temperature.

CoTMPP700 [4] [5] (University of New Mexico): 0.5 g of CoTMPP (Aldrich) is dissolved in 100 ml of tetrahydrofuran. 0.5 g of CAB-O-SIL (325 m^2g^{-1}) amorphous fumed silica (Cabot) is added to the solution. The tetrahydrofuran evaporates, inducing precipitation of the catalyst precursor on the silica template. The templated material was then

pyrolyzed at 700˚C under N_2 for 4 h. Finally, the silica template is removed with a KOH wash and the material is dried.

The second approach (ii) uses a metal salt as the exclusive metal precursor and a N-containing molecule as the exclusive N source. No pre-existing carbon support is used. The pyrolysis is carried out under inert atmosphere. Catalysts investigated in the present paper that correspond to approach (ii) are GAdFeCu and DAL900A.

GAdFeCu [6] (OMTRI): Glucose ($C_6H_{12}O_6$), adenine ($C_5H_5N_5$), Fe^{II} gluconate ($C_6H_{12}O_7$) dihydrate and Cu^{II} gluconate are ground together. The molar ratio of glucose to adenine, and that of Fe^{II} to Cu^{II}, are one. The sum of Fe and Cu contentsis 1 wt %. The mixture is heated to 150˚C in air for 24 h for glucose dehydration. After grinding, the powder is heated under Ar at 5˚C min^{-1} up to 1000˚C and held there for 2h. The catalyst obtained is ground and acid-washed in boiling 0.5 M H_2SO_4 for 1h, followed by filtering, washing with high-purity water, and drying under vacuum at room temperature.

DAL900A [7] [8] (Dalhousie Univ.): Mesoporous silica is used as a template [9]. 1g mesoporous silica (Koestrosorb 1015, donated by Chemiewerk Bad Koestritz, Germany) with μm-sized particles is impregnated with 1 mL of an aqueous solution of iron[III] chloride (0.1 M). The mixture is dried at 80˚C for 12h. Then the impregnated silica (1 g) is loaded with 1 mL of pyrrole (C_4H_5N, density 0.97). To polymerize the pyrrole, the pyrrole-loaded silica is exposed to HCl vapour. After complete polymerization monitored by thermal gravimetry, the sample is carbonized under Ar flow by heating the oven at 2ºC min^{-1} to 900ºC and then held there for 2h. To remove silica and non-activated iron,

the sample was treated with a solution of 5 % HF for 1h then washed with 40 % HF. The sample was collected with filter paper, washed with d. water and finally dried at 100ºC.

A third approach (iii) consists in performing a second heat treatment under a reactive atmosphere to catalysts that have undergone a first heat treatment under inert atmosphere (approaches (i) and (ii)). The reactive atmosphere could be oxidative (O_2, CO_2) or reductive (NH_3, N_2/H_2). Catalysts synthesized according to that approach are UK63, UK65 and DAL900C. The two first are already listed under approach (i).

DAL900C (Dalhousie University): One gram of the catalyst DAL900A is impregnated with 2 ml of Iron II acetate solution (0.018 M). After drying, the powder is heated from 20°C to 400°C at 25°C min^{-1} under Ar. After a hold at 400 °C for 30 min, the gas stream is switched to NH_3 and the furnace is heated to 900 °C at 25°C min^{-1}. The dwell time is 40 min at 900 °C. The sample is cooled down under Ar. The weight loss during NH_3 heat treatment is 47 wt %.

The fourth approach (iv) uses a metal salt as the exclusive metal precursor and NH_3 under pyrolysis as the exclusive N precursor. The carbon precursors are carbon blacks.

FC280 [10] [11] (INRS): 6.24 mg of iron acetate is impregnated in water solution on 1 g of a pristine furnace black (Sid Richardson Carbon Company, BET area 63 m^2g^{-1}) to result in a nominal Fe content of 0.2 wt %. The solution is stirred 2 h followed by evaporation of about ¾ of the liquid on a heating plate and then dried overnight in an oven at 80˚C. The sample is heat-treated at 950˚C under NH_3 for 40 min. The procedure to control precisely the duration of 40 minutes at 950˚C is described in [12]. The duration of 40 minutes was

found to give the maximum activity with that specific carbon black [11]. The catalyst is cooled down under Ar.

M786 (INRS): 0.5 g of carbon black Black Pearls 2000 (1380 m^2g^{-1}), 0.5 g of perylene tetra-carboxylic dianhydride (PTCDA, $C_{24}H_8O_6$) and 6.24 mg iron acetate (0.2 wt % Fe in the initial mixture of Black Pearls + PTCDA) are mixed together in a steel vial filled with N_2 by planetary ball milling (20 beads with a total mass of 20 g). The ball milling is crucial to intimately fill the pores present in Black Pearls by PTCDA which acts as disordered carbon. Then, the mixture is heat-treated at 1050˚C under NH_3 for 5 min. The procedure to control precisely the duration of 5 minutes at 1050˚C is the same as in [12].

C. Other ink formulations tested for RDE

For the catalysts GAdFeCu and CHb200900, two ink recipes were tested: the usual NNMC recipe described in section II.2.2 and an ink recipe previously used by Maruyama [3]. The formulation of the latter is 10 mg of catalyst, 1 mg of carbon black, 100 μL of 5 wt % Nafion in alcohol and 100 μL of distilled water. The ink is then mixed as described above for the usual NNMC ink. A 3 μL-aliquot is dropped on the glassy carbon. This results in a catalyst loading of 765 μg cm^{-2}. The results on GAdFeCu and CHb200900 were the same with both inks and only the RDE graphs obtained with the usual NNMC ink are reported.

For the catalysts UK63 and UK65, two ink recipes were tested: the usual NNMC recipe described in section II.2.2 and an ink recipe used at the Helmholtz-Zentrum Berlin (HZB ink). For the latter, a diluted Nafion solution is first prepared by mixing 14.4 mL of ethanol, 14.4 mL of water and 1.125 mL of a 5wt% Nafion solution (Aldrich). Then 3

mg of NNMC is dispersed in 200 μL of the diluted Nafion solution. The ink is then mixed as the usual NNMC ink. The overall formulation of the ink is 10 mg of NNMC, 25 μL of a 5 wt % Nafion solution (Aldrich), 321 μL of ethanol and 321 μL of d. water. A 5-μL aliquot is deposited on the glassy carbon, resulting in an NNMC loading of 380 μg cm^{-2}. Results obtained with the usual NNMC ink and with the above HZB ink were identical in term of mass activity of the catalysts UK63 and UK65.

For two catalysts made at INRS that were very similar to FC280, the HZB ink was also tested. Surprisingly, for these particular catalysts, the mass activity was smaller by a decade when using the HZB ink compared to as using the usual ink recipe described in section II.2.2. The main difference between the two inks is the Nafion content for 10 mg of NNMC: 95 μL for the usual ink and only 25 μL for the HZB ink.

For the catalyst CoTMPP700, the usual NNMC ink was also tested on CoTMPP700 and resulted in same mass activity but the Tafel slope was confined to a smaller potential range, which motivated the choice of this alternative ink formulation.

D. Definition of target mass activity for NNMC in RDE at 20˚C.

The experimental curve E vs log (I_M) for Pt/C (Fig.1B) was fitted to a Tafel law of the type

$$I_M = I_M^* \cdot \exp\left[\frac{-\ln 10}{\text{Tafel}}\left(E_{\text{vs RHE}} - E^*\right)\right] \qquad \text{Eq. S2}$$

Where I_M is the mass activity (A per g carbon in the Pt/C catalyst), Tafel is the Tafel slope, and I_M^* is the mass activity at potential E^*. For an easy comparison of today's NNMC activity with Pt activity, the potential E^* is chosen to be 0.8 V. This potential (almost equal to 0.5 V vs. SCE at pH 1) has previously been used to report the kinetic activity of NNMC in RDE and also in fuel cell [12] [13]. The 46 % Pt/C catalyst gives $I_M^* =$ 2536 A per g carbon with a Tafel slope of 64 mV/decade. The targeted ORR-activity for NNMC is to first reach 1/10$^{\text{th}}$ of the activity of Pt/C catalyst [1]. Thus, under the assumption that NNMC and Pt/C behave similarly with temperature, we derived a target-curve for NNMC mass activity in RDE at room temperature defined by Eq.S2 with $E^* =$ 0.8 V vs RHE, $I_M^* = 253.6$ Ag^{-1} NNMC and a Tafel slope of 64 mV/decade. This target curve is plotted in Fig.1B as dash-dot.

The corresponding target Faradaic current density (curve (b) in Fig.1A) was then simply derived with the Koutecky-Levich equation (section II.2.4) and using $I_{\text{lim}} = -6$ mA cm^{-2} (4 electron ORR at 1500 rpm) and with $m_{\text{catalyst}} = 460$ µg cm^{-2}. The loading 460 µg cm^{-2} was chosen since it is the loading experimentally employed for the most active catalysts in RDE (UK63 and UK65).

E. Nature of the red-ox peaks seen in N_2 cyclic voltammetry of RDE or PEMFC.

Several of the NNMC show red-ox peaks, either broad (GAdFeCu, CHb200900) or more clearly defined (UK65) (Fig.2A). The position of the red-ox peaks is catalyst-dependent. The reduction peak cannot be ascribed to ORR since the solution is O_2-free. The red-ox peaks are stable upon cycling and thus cannot be due to the free Fe^{II}/Fe^{III} red-ox. The latter has a thermodynamic equilibrium potential of 770 mV vs. NHE (830 mV vs. RHE at pH 1) which is much higher than the red-ox potentials observed here. The red-ox peaks can be ascribed to either (i) surface functional groups containing C,N,O or H atoms that are created during the heat treatment step necessary to synthesize the catalysts or created later upon exposure to air, or ascribed to (ii) stabilized iron linked to nitrogen atoms. For case (i), the surface species responsible for the red-ox peaks can be for example of quinone/hydroquinone nature. This is a vast family whose red-ox peaks can show very different positions in the voltammogram (pgs. 306-315 in [14]). Red-ox peaks appear even on a glassy carbon electrode upon electrochemical oxidation [15]. For case (ii), iron stabilized by ligands in $Fe-N_4$ chelates like phthalocyanines or porphyrins shows one or two pairs of red-ox peaks (non heat-treated chelates) [16][17] . In order to distinguish between Fe-containing and Fe-free surface groups as the origin of the red-ox peaks, the N_2-CVs were recorded at pH 1 and at pH 4 for the catalysts UK65 and CHb200900 and compared to the N_2-CVs of a non-heat-treated iron phthalocyanine adsorbed on Vulcan ($200-220$ m^2g^{-1}). Protons are involved in quinone/hydroquinone red-ox groups but a priori not in Fe-based red-ox groups. Figure S1 presents these N_2-CVs. At pH 4, both the

red-ox peaks of UK65 and of CHb200900 are absent. Also, the shape of the N_2-CVs at pH 4 is almost a perfect square wave, as expected for a potential-independent capacitance of the surface. It seems therefore that, for a given catalyst, the difference in area between the N_2-CV at pH 1 and that at pH 4 is due to an important contribution of pseudo-capacitance brought, at pH 1, by metal-free surface groups like quinine structures. For UK65, this pseudo-capacitance seems to be not only present at potentials near to the red-ox peaks but extends at all scanned potentials. This could be due to many different red-ox sites. The capacitance at pH 4 is free of pseudo-capacitance and is therefore expected to be proportional to the catalyst specific area. The BET area of CHb200900 is 715 m^2g^{-1} while that of UK65 is 818 m^2g^{-1}. This is in perfect accordance with their slight difference in capacitive currents at pH 4. Also, for a same electrode, the disappearance of the red-ox peaks when the electrode is transferred from a pH 1 to a pH 4 electrolyte is reversible; i.e. when the same electrode is put back in pH 1 electrolyte, the red-ox peaks re-appear with the same intensity. Thus, it is obvious that the red-ox system is strongly bonded to the carbon surface and the red-ox system at pH 1 is not due to metal dissolution.

The lower panel of Fig.S1 shows the response of the Fe phthalocyanine adsorbed on Vulcan. At pH 1, two pairs of red-ox peaks are observed, one at 628/662 mV vs. RHE and a second one at 137/172 mV vs. RHE. At pH 4, the two pairs of red-ox peaks are still observed but broader and with a smaller intensity. The positions are 685/775 mV vs. RHE and -50?/140 mV vs. RHE. If the red-ox pairs had a fixed potential in an SCE scale, their position on a RHE scale should have increased by 3 pH units x 60 mV/decade = +180 mV. For the red-ox labelled 1 (Fig.S1) the position on the RHE scale shifted by +110 mV for the oxidation peak and only by +60 mV for the reduction peak. For the red-

ox 2, its position did not shift upward but slightly downward on the RHE scale. This means that the positions of the Fe phthalocyanine red-ox 1 and 2 are not fixed in an SCE scale and that their dependence to a change in pH differs from one another. This has been previously shown for a tetra-sulfonated Fe phthalocyanine [16]. Moreover, the same authors showed that the red-ox labelled 1 had a shift of +60 mV/pH unit but only at pH > 4.5 (pH 4 is close to pH at which Fe starts to form hydroxides). At pH < 4, the shift per pH unit was < +60 mV, which is in very good agreement with our present measurement on Fe phthalocyanine. This means that the red-ox labelled 1 involves a proton. Accordingly, the red-ox reaction proposed by Zagal for red-ox 1 of the Fe phthalocyanine was $Fe^{III}OH + H^+ + e^- \leftrightarrow Fe^{II}OH_2 + H_2O$.

Thus, as seen in Fig.S1, the red-ox peaks of, on one side, the Fe-phthalocyanine and on another side, of UK65 and CHb200900, react completely differently to the pH change from 1 to 4.

In conclusion the red-ox peaks observed on UK65 and CHb200900 are assigned mainly to <u>iron-free</u> surface groups which are involved in a proton coupled red-ox reaction. A possible structure is the quinone-hydroquinone red-ox couple which is often observed on carbon surfaces. Non perfect square-wave form of N_2-CVs measured at pH 1 for all NNMC (Fig.2) is probably due to many red-ox couples covering a wide potential range.

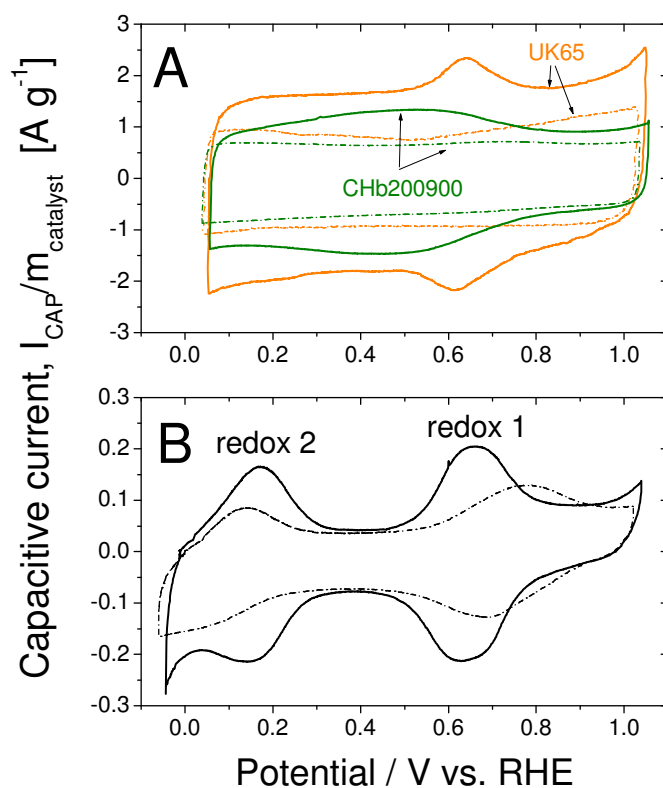Figure S1: Voltammetry in N_2 at pH 1 and 4 of chosen NNMC in RDE.

N_2-saturated electrolytes of pH 1 (solid line) and of pH 4 (dash-dot line).

At pH 4, supporting salt 0.1 M K_2SO_4 was used. Scan rate 10 mVs^{-1}.

A: catalysts UK 65 (orange) and CHb200900 (green), usual NNMC ink and loading 800 μg cm^{-2}.

B: Non-heat-treated iron phthalocyanine adsorbed on Vulcan. Loading 443 μg (Fe-phthalocyanine and vulcan) cm^{-2}. The ink formulation is 12 mg of Fe phthalocyanine, 50 mg of Vulcan XC72-R, 2500 μL of water and 2500 μL of a 5wt% Nafion solution.

F. SEM pictures
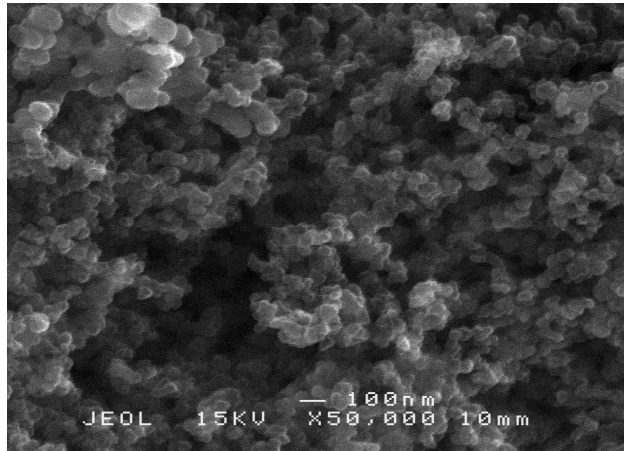
FC280. Enlargement 50k. Average particle size 40 nm and agglomerate size 400 nm
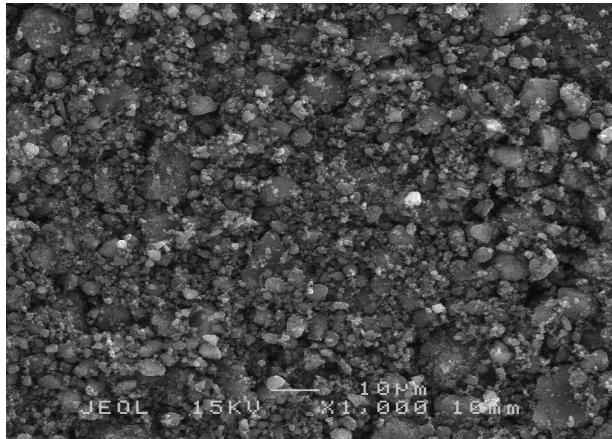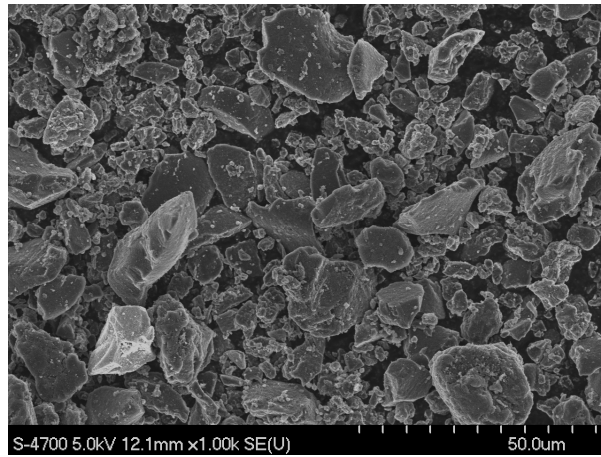

M786. Enlargement 1k. Average particle size 3 µm.
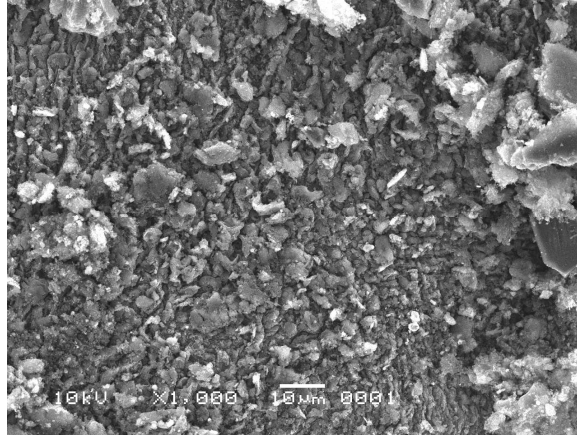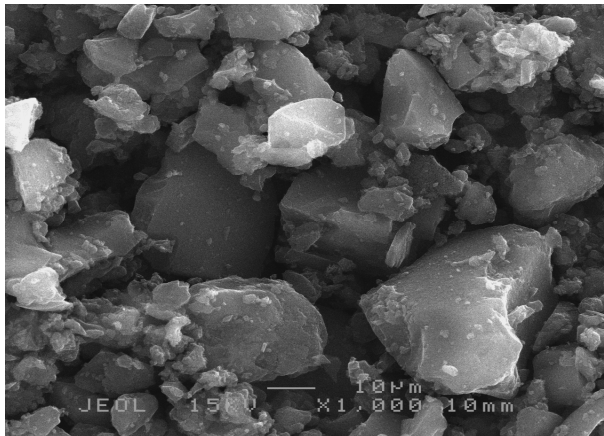
CHb200900. Enlargement 1k. Average particle size 10 μm.
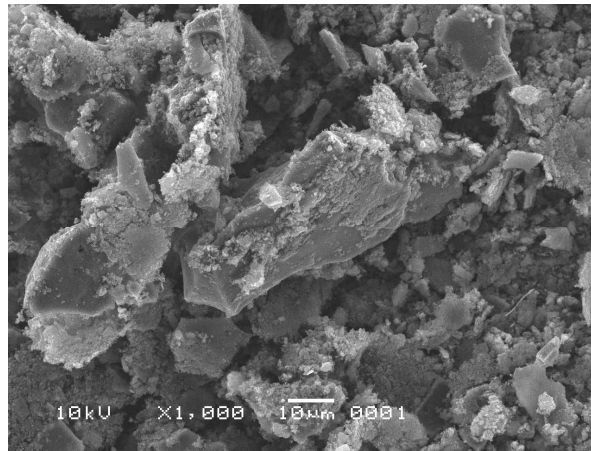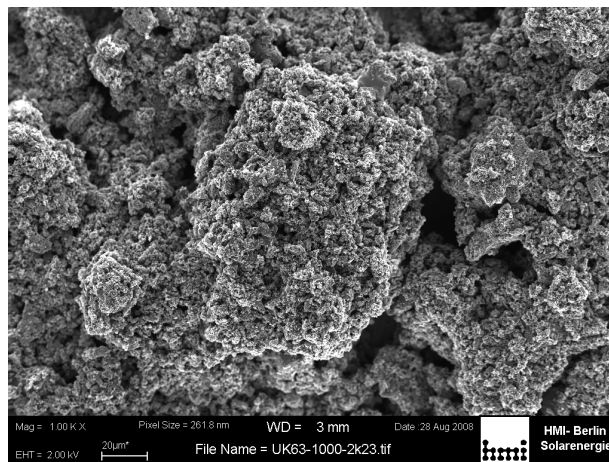

GAdFeCu. Enlargement 1k. Average particle size 20 μm.
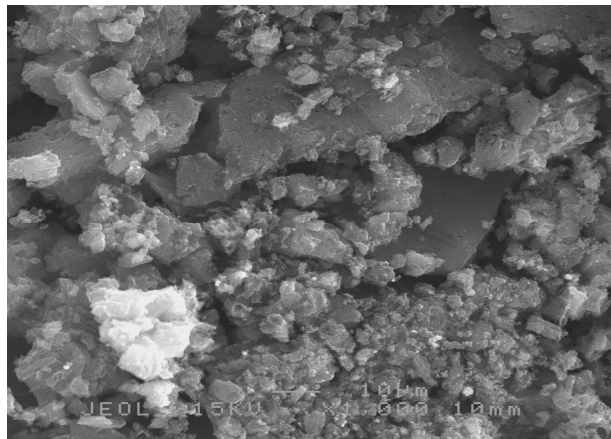
CoTMPP700. Enlargement 1k. Average particle size 30 μm.
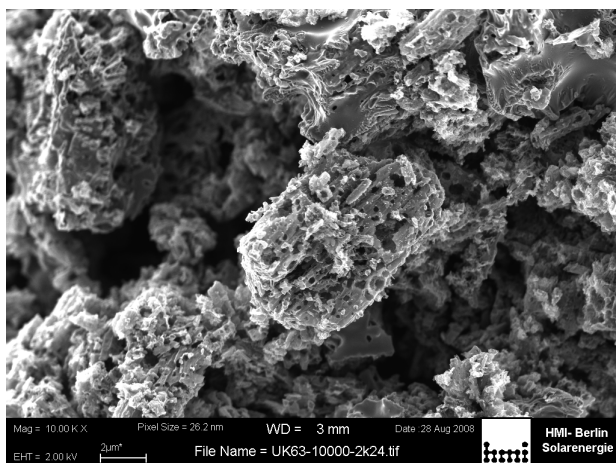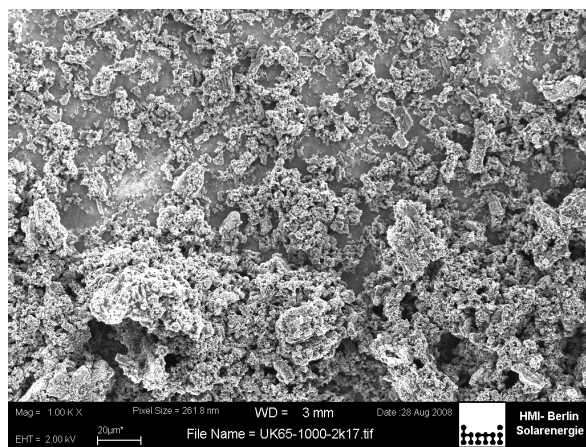
DAL900A. Enlargement 1k. Average particle size 20 μm.

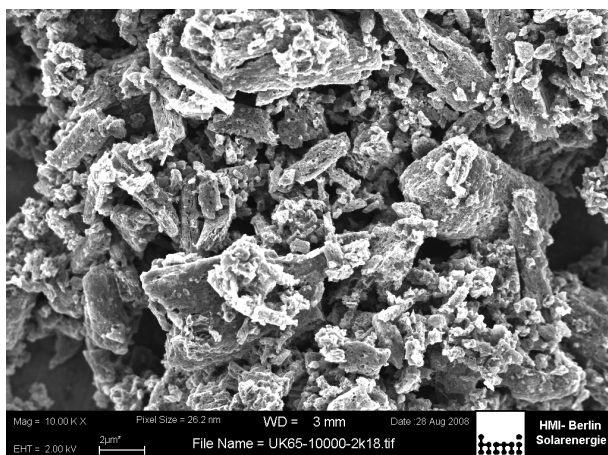DAL900C. Enlargement 1k. Average particle size 20 μm.

UK63. Enlargement 1k.

UK63. Enlargement 10k. Average particle size 7 μm.

UK65. Enlargement 1k.

UK65. Enlargement 10k. Average particle size 4 μm.

References

(1) Gasteiger, H. A.; Kocha, S. S.; Sompalli, B.; Wagner, F. T. *Appl Catal B-Environ* **2005**, *56*, 9.

(2) Koslowski, U. I.; Abs-Wurmbach, I.; Fiechter, S.; Bogdanoff, P. *J. Phys. Chem. C* **2008**, *112*, 15356.

(3) Maruyama, J.; Okamura, J.; Miyazaki, K.; Uchimoto, Y.; Abe, I. *J. Phys. Chem. C* **2008**, *112*, 2784.

(4) Olson, T. S.; Chapman, K.; Atanassov, P. *J. Power Sources* **2008**, *183*, 557.

(5) Ziegelbauer, J. M.; Olson, T. S.; Pylypenko, S.; Alamgir, F.; Jaye, C.; Atanassov, P.; Mukerjee, S. *J. Phys. Chem. C* **2008**, *112*, 8839.

(6) Maruyama, J.; Abe, I. *Chem. Comm.* **2007**, *27*, 2879.

(7) Garsuch, A.; d'Eon, R.; Dahn, T.; Klepel, O.; Garsuch, R. R.; Dahn, J. R. *J. Electrochem. Soc.* **2008**, *155*, B236.

(8) Garsuch, A.; McIntyre, K.; Michaud, X.; Stevens, D. A.; Dahn, J. R. *J. Electrochem. Soc.* **2008**, *155*, B953.

(9) Garsuch, A.; Sattler, R. R.; Witt, S.; Klepel, O. *Microporous and Mesoporous Materials* **2006**, *89*, 164.

(10) Charreteur, F.; Jaouen, F.; Ruggeri, S.; Dodelet, J. P. *Electrochim. Acta* **2008**, *53*, 2925.

(11) Charreteur, F.; Ruggeri, S.; Jaouen, F.; Dodelet, J. P. *Electrochim. Acta* **2008**, *53*, 6881.

(12) Jaouen, F.; Lefèvre, M.; Dodelet, J. P.; Cai, M. *J. Phys. Chem. B* **2006**, *110*, 5553.

(13) Jaouen, F.; Dodelet, J. P. *Electrochim. Acta* **2007**, *52*, 5975.

(14) Kinoshita, K. *Carbon, electrochemical and physicochemical properties*; John Wiley & Sons: New-York, 1988.

(15) Maruyama, J.; Abe, I. *Electrochim. Acta* **2001**, *46*, 3381.

(16) Zagal, J.; Bindra, P.; Yeager, E. *J. Electrochem. Soc.* **1980**, *127*, 1506.

(17) Gupta, S.; Fierro, C.; Yeager, E. *J. Electroanal. Chem.* **1991**, *306*, 239.